Experimental Neurology 320 (2019) 112986

Contents lists available at ScienceDirect

Experimental Neurology

journal homepage: www.elsevier.com/locate/yexnr

Research Paper

Activation of the spinal neuronal network responsible for visceral control during locomotion

Natalia Merkulyeva[a,b,c], Vsevolod Lyakhovetskii[a,b], Aleksandr Veshchitskii[a], Elena Bazhenova[a,c], Oleg Gorskii[a,b,c], Pavel Musienko[a,b,c,d,*]

[a] Pavlov Institute of Physiology RAS, Saint-Petersburg, Makarov emb., 6, 199034, Russia
[b] Russian Research Center of Radiology and Surgical Technologies, Ministry of Health of the RF, Saint-Petersburg, poselok Pesochnyy, Leningradskaya str., 70, 197758, Russia
[c] Institute of Translational Biomedicine, Saint-Petersburg State University, Saint-Petersburg, Universitetskaya emb., 7-9, 199034, Russia
[d] Children's Surgery and Orthopedic Clinic, Department of Non-pulmonary Tuberculosis, Research Institute of Phthysiopulmonology, Saint-Petersburg, Politekhnicheskaya str., 32, 194064, Russia

ARTICLE INFO

Keywords:
C-fos
Electrical epidural stimulation
Spinal cord
Locomotor network
Parasympathetic neurons
Bladder function
Cat

ABSTRACT

It has been established that stepping of the decerebrate cat was accompanied by involvement of the urinary system: external urethral sphincter (EUS) and detrusor muscle activation, as well as the corresponding increase of the intravesical pressure. Detrusor and EUS evoked EMG activity matched the limbs locomotor movements. Immunohistochemical labeling of the immediate early gene *c-fos* expression was used to reveal the neural mechanisms of such somatovisceral interconnection within the sacral neural pathways. Study showed that two locomotor modes (forward and backward walking) had significantly different kinematic features. Combining the different immunohistochemical methods, we found that many *c-fos*-immunopositive nuclei were localized within several visceral areas of the S2 spinal segment which matched the sacral parasympathetic nucleus and dorsal gray commissure. Cats stepping backward had 4-fold more *c-fos*-immunopositive nuclei within the ventrolateral part of the sacral parasympathetic nucleus apparently correspondent to the "lateral band" contained cells controlling bladder function. The present work provides the direct evidences of visceral neurons activation depending on the specific of locomotor pattern and confirms the somatovisceral integration carrying out on the spinal cord level.

1. Introduction

A severe spinal cord injury (SCI) leads not only to disabilities in the sensorimotor control and permanent paralysis but also to the autonomic function's impairment including reflex and voluntary control of storage and voiding of the urine (Guttmann and Whitteridge, 1947; de Groat, 1995; de Groat and Yoshimura, 2010; Gomez-Amaya et al., 2015). Epidural electrical stimulation (ES) of the spinal cord has been shown to be high effective for recovery of locomotor abilities in both humans and animals with SCI (Minassian et al., 2004; Gerasimenko et al., 2008; Musienko et al., 2009). It was demonstrated recently that ES can affect the control of lower urinary tract (LUT) system (Gad et al., 2014, 2016), and multi-system neurorehabilitation combining electro-chemical activation of spinal circuitry and motor training not only can restore walking capacities but also counteracts the formation of an overactive neuropathic bladder (Horst et al., 2013).

Spinal neurons receive an afferent input from the pelvic organs and responsible for the control of smooth and striated muscles of LUT system. They are distributed in a thoraco-lumbar (sympathetic cells) and in sacral (parasympathetic cells and motoneurons of urethral sphincter) regions (de Groat et al., 2001). It was shown that both functions, urine storage and release, require an intact innervation from the sacral spinal cord while lumbar sympathetic innervation is mostly important for increasing the range of continence (Bahns et al., 1986). From other side, the neuronal circuitry responsible for locomotion is located within the lumbosacral spinal cord organizing a central pattern generator (CPG) controlling the rhythm generation and pattern formation during hindlimbs stepping (Grillner, 1980). CPG networks are

Abbreviations: ES, electrical stimulation; FOS+, *c-fos*-positive; FW, forward locomotion; BW, backward locomotion; SPN, sacral parasympathetic nucleus; DGC, dorsal gray commissure; HRP, horseradish peroxidase; NOS, NO-synthase (nitric oxide synthase); CL, centrolateral area; VL, ventrolateral area; PC, pericanal area; DL, dorsal lateral area; DM, dorsal medial area; LUT, low urinary tract; CPG, central pattern generator; SCI, spinal cord injury; EUS, external urethral sphincter

* Corresponding author at: Institute of Translational Biomedicine, Saint-Petersburg State University, Saint-Petersburg, Universitetskaya emb., 7-9, 199034, Russia.
E-mail address: pol-spb@mail.ru (P. Musienko).

https://doi.org/10.1016/j.expneurol.2019.112986
Received 8 February 2019; Received in revised form 19 May 2019; Accepted 25 June 2019
Available online 26 June 2019
0014-4886/

widely distributed over the lumbosacral enlargement (Merkulyeva et al., 2018); and their elements controlling the hindlimbs foot and fingers muscles are located in the close relation to the region containing the bladder network (segment S2) (Vanderhorst and Holstege, 1997).

Since the locomotor and LUT systems seem structurally and functionally interconnected, we can propose that somatic and visceral spinal neural populations can be combined into a single network (Gad et al., 2014, 2016). *The aim of the present work* is to show the bladder neuronal pathways involvement in the activity during activation of the locomotor network by the ES, and to find the distribution pattern of the activated visceral neurons in sacral region.

Decerebrate cat model was used to perform the simultaneous recordings of the locomotor and visceral signals. This unique model allowed to induce well controlled reproducible locomotor behaviors (Shik and Orlovsky, 1976; Whelan, 1996) and investigate the specific role of the spinal and brain stem networks in regulation of physiological functions including urinary system activity (Kruse and De Groat, 1993; Shefchyk and Buss, 1998), in non-anesthetized conditions without voluntary control and forebrain input. We combined the functional testing with the following immunohistochemical evaluation of the activated neurons expressing immediately early gene *c-fos* (Dragunow and Faull, 1989; Presley et al., 1990; Dai et al., 2005; Ichiyama et al., 2008; Courtine et al., 2009; Duru et al., 2015); and revealing of the neurons expressing NO-synthase (Nadelhaft et al., 1980; Morgan et al., 1979) and Ca^{2+}-binding protein calretinin (Ren and Ruda, 1994) to attribute the activated cells to the visceral pathways.

2. Materials and methods

2.1. Subjects

Fifteen adult cats of either sex weighing 2.5–4.0 kg were used for this study. All experimental procedures were approved by the Ethics Commission of the Pavlov Institute of Physiology. Experiments were performed in accordance with requirements of Council Directive 2010/63EU of the European Parliament on protection of animals used in experimental and other scientific purposes. Eight animals were used only for the registration of the LUT activity, and other seven animals were used for the *c-fos* experiment.

2.2. Surgical procedures and epidural stimulation

All cats were deeply anesthetized with a mixture of Isoflurane (2–4%) and Oxygen gas. The trachea was cannulated, and carotid arteries were ligated. The animals were decerebrated at the precollicular-postmammilar level.

The intravesical pressure was measured using cystometry sensor (Fig. 1A). Following a midline abdominal incision, a catheter (Perifix 401, 18G) was introduced through the apex of the bladder and secured using a 6.0 Ethilon suture (Ethicon, New Brunswick, NJ). The catheter was connected to a solid state pressure transducer (MLT0670, AU) and through syringe pump (ZOOMED SN-1600 V, RU), the room temperature 0.9% saline solution was injected. Bladder volume was maintained at low level (5–7 ml) to prevent reflex bladder contractions unrelated to the stepping. To detect an electromyographic (EMG) activity of the detrusor and external urethral sphincter (EUS), the bipolar EMG electrodes (0.2 mm flexible stainless-steel Teflon-insulated wires; AS632, Cooner Wire, Chatsworth, CA) were implanted. The EMG electrodes signal was differentially amplified (A-M Systems, model 1700, US, bandwidth of 10 Hz to 5 kHz), digitized at 20 kHz with a National Instrument A/D board, rectified, and integrated by computer programs.

A laminectomy was performed in the lumbar area. Anesthesia was terminated after the surgical procedures, and the experiments were initiated 2–3 h thereafter. During the experiment, the rectal temperature, electrocardiography and breathing rate of the animal were continuously monitored to control stable vital conditions of the animals.

Animals were fixed in a rigid frame (Fig. 1A). Active locomotion was evoked by the ES of the segments L5-L7 of the spinal cord (Fig. 1B) using the ball electrode (d = 0.5 mm), the indifferent ground wire electrode inserted into the paravertebral muscles. Electrical stimulation was applied with a stimulator (A-M Systems, model 2100 isolated pulse stimulator, US). This method was extensively used earlier to trigger locomotor circuitry in decerebrated cat model and investigate different aspects of neuronal control of the walking (Gerasimenko et al., 2008; Iwahara et al., 1992; Musienko et al., 2012). In accordance to previous study (Musienko et al., 2007) parameters of ES were as follows: frequency, 5 Hz; pulse duration, 0.3–0.5 ms; and electrical current, 220–300 μA. The direction of locomotion was determined by the direction of the treadmill belts. Passive locomotion was realized by the learned operator by the way used previously (Gerasimenko et al., 2009): animal's hindlimbs were moved manually forward and backward imitating the real locomotor movements.

For the *c-fos* experiment, animals had periodical sessions (1–2 min every 4–5 min during 1.5–2.0 h) of the ES evoked stepping in FW (cats Fw1, Fw2, Fw3) or BW (cats Bw1, Bw2, Bw3) direction. The control cat was subjected to the same surgical procedures as experimental ones, but the ES stimulation period (and corresponding stepping activity) was much shorter – 30 min. During this period cat was stimulated in segments L5, L6, L7 (approx. 5 min per segment) and stepped both FW and BW.

2.3. Kinematic analysis

To characterize the support surface of the foot, the side view of the walking cat was video recorded (25 frames/s) and analyzed frame-by-frame. The foot length was calculated at moment when the hindlimb maximally contacts the surface. The anterior/posterior (A-P) limb movements (by means of two mechanical sensors attached to the ankles) were also recorded. The kinematic signals were amplified and digitized at 20 kHz.

2.4. Analysis of the LUT activity

LUT activity was analyzed using two approaches: (1) EMG activity of the detrusor and EUS, and (2) cystometric curve. The signal from the EUS was filtered using bandpass filter at 100–2000 Hz range; the detrusor smooth muscle signal was filtered at 10–40 Hz since was previously obtained (Fry et al., 1998). The delta of EMG activity in EUS and detrusor muscles was calculated as the difference between maximal and minimal percentage value of activity of these muscles obtained within locomotor cycle. A maximal value of the cystometric signal was taken into account for the assessment of the intravesical pressure during different locomotor tasks.

2.5. Perfusion and dissection

At the end of experiments, animals were deeply anesthetized with Isoflurane (5%), and then perfused transcardially with 0.9% NaCl (2.0 L), followed by 4% paraformaldehyde (2.0 L). After perfusion, the spinal cord was removed from the spine and stored in 20% and 30% sucrose. The detailed dissection of vertebrae, roots and spinal cord was performed for determination the exact level of spinal cord stimulation, laminectomies and spinal segments for following immunohistochemical analysis. The lumbosacral cord was divided into segments based upon the grouping of the dorsal rootlets (Shkorbatova et al., 2018). Sacral segment S2 was cut on a freezing microtome into 50 μm transverse slices. Five equally spaced sections were processed for *c-fos* immunohistochemical protocol. Adjacent slices were used for the either calretinin, or NOS staining.

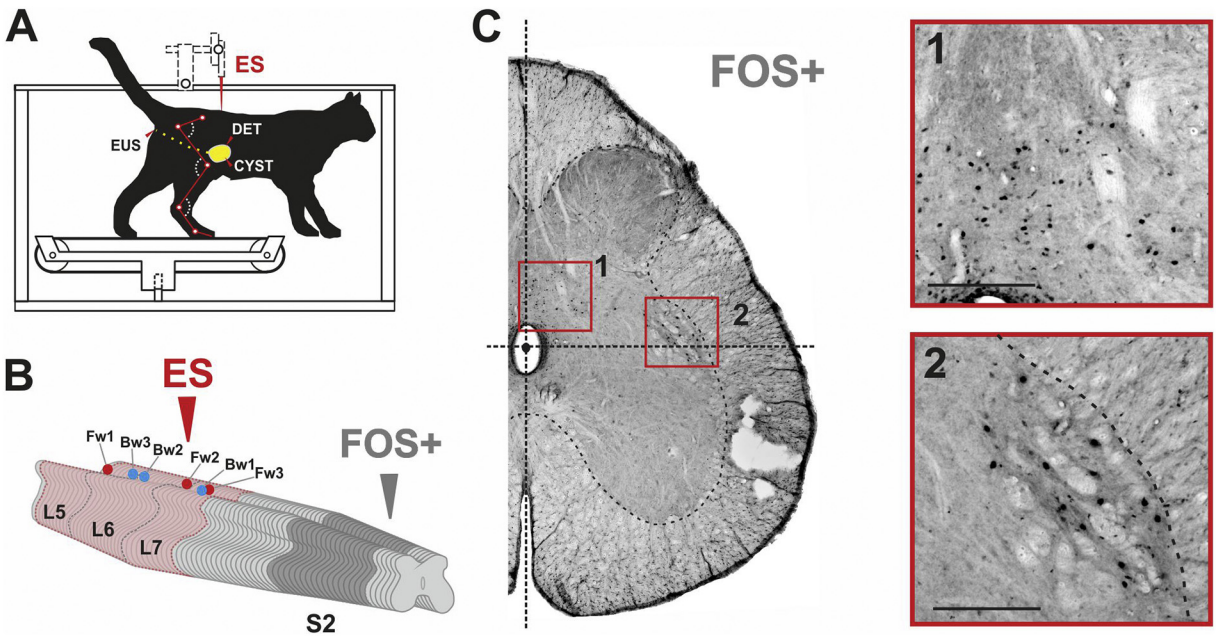

Fig. 1. Experimental setup. A – the cat was fixed in a rigid frame. The hindlimbs were positioned on the treadmill. An intra-bladder pressure (cystometry, CYST) and EMG of the detrusor muscle (DET) and external urethral sphincter (EUS) were recorded. The hindlimb joints are marked by white dots, bones – by red lines. Walking of the hindlimbs was evoked by the epidural stimulation (ES). B – location of the ES points (L5-L6-L7 segments) and region of the c-fos-labelling (FOS +) in the S2 segment of the spinal cord. Red and blue spots mark the location of the ES points for the individual cats, stepping forward (Fw) and backward (Bw). C – a distribution of the FOS + nuclei at the transverse slice of the segment S2. Groups of the FOS + nuclei are presented in enlarged inserts 1 and 2. Two crossed dotted lines mark the central canal. Calibration marker at C is 200 μm. (For interpretation of the references to colour in this figure legend, the reader is referred to the web version of this article.)

2.6. Immunohistochemical staining

Detailed procedures of the immunostaining were described previously (Merkulyeva et al., 2016). Briefly, after unmasking in 1% $NaBH_4$, endogenous peroxidase activity blocking, and blocking of the non-specific staining by incubation in 10% normal goat serum (NGS, Vector Laboratories, Peterborough, UK), slices were incubated in primary antibodies: polyclonal anti-C-fos anti-rabbit (Millipore, USA, PRID: AB_2106755, 1:10000 dilution); polyclonal anti-Calretinin anti-rabbit (Millipore, USA, PRID: AB_2068506, 1:5000 dilution); polyclonal anti-NO-synthase anti-rabbit (Millipore, USA, PRID: AB_91824, 1:1000 dilution) for 70 h at +4 °C. Then, the slices were incubated in biotinylated secondary antibodies: goat anti-rabbit IgG (Vector Laboratories, UK, PRID: AB_2313606, 1:600 dilution), and goat anti-mouse IgG (Vector Laboratories, UK, PRID: AB_2336171, 1:600 dilution) for 1 day, in avidin-biotin horseradish-peroxidase complex (ABC Elite system, Vector Laboratories, Peterborough, UK) for 1 h, and in a mixture of diaminobenzidine (DAB), NiCl and 0.03% H_2O_2 (Vectastain DAB kit, Vector Laboratories, Peterborough, UK) for 15 min. Thereafter slices were dried, dehydrated in alcohol, and coverslipped in Bio Mount (Bio-Optica, Milano, Italy).

2.7. Image acquisition and morphological data analysis

Images were acquired with an Olympus microscope (Olympus Corporation, Tokyo, Japan, a 10× objective) using a Nikon photo camera (Nikon Corporation, Tokyo, Japan). Nuclei labelled with an anti-C-fos antibody (FOS + nuclei) were detected as dark oval-to-round shaped loci (Fig. 1C). All images were then processed with free software from Fiji (Schindelin et al., 2012), adjusting for brightness, contrast, and sharpness to make contoured images. While counting images, all FOS + nuclei were marked with dots of the same size. For demonstration purposes, transverse slices were combined into single "total slice", using gray matter contours as a landmark. All FOS + nuclei were superimposed at this slice, for every animal. Left and right sides of the spinal cord were analyzed separately, for all cats.

2.8. Statistical analysis

Data presented as mean ± SEM. Statistical significance was assessed using the Mann-Whitney test.

3. Results

3.1. Bladder activity during stepping

We have used the precollicular-postmammilar model of decerebrated cat (n = 7) to monitor both locomotor and LUT systems. Epidural spinal cord stimulation was applied to trigger spinal locomotor network (Iwahara et al., 1992). It was found that after few seconds ES not only initiates the stepping hindlimb movements FW and BW depending on the direction of the treadmill belt (Musienko et al., 2012), but also facilitates the activity of urinary system (see detrusor, EUS and cystometric signals on Fig. 2A). Cessation of ES discontinued the locomotion and gradually returned the activity of urinary system to initial level. The peak-levels of the cystometric signals were around 20–30 mmHg (Figs. 2A and 3D) that is in agreement with the literature data (Shefchyk and Buss, 1998).

The detrusor and EUS activity revealed during ES-evoked locomotion was in the burst-like mode (Fig. 2A). To check whether these EMG bursts were actually influenced by the locomotor movements but not the ES *per se,* we analyzed EMG activity in comparison to the pattern of ES and the hindlimbs kinematics. Detrusor and EUS bursts in activity were not followed the frequency of ES but well matched the rhythm of limbs movements (Fig. 2A). The activity of both detrusor and EUS was analyzed during passive locomotion non-related to the electrical stimulation. It was noticed that even without ES, the detrusor and EUS EMG signals were interrelated with the locomotor rhythm (Fig. 2B).

The analysis of relationship between the LUT activity and the locomotor cycle is presented at Fig. 3. As shown on example from one cat

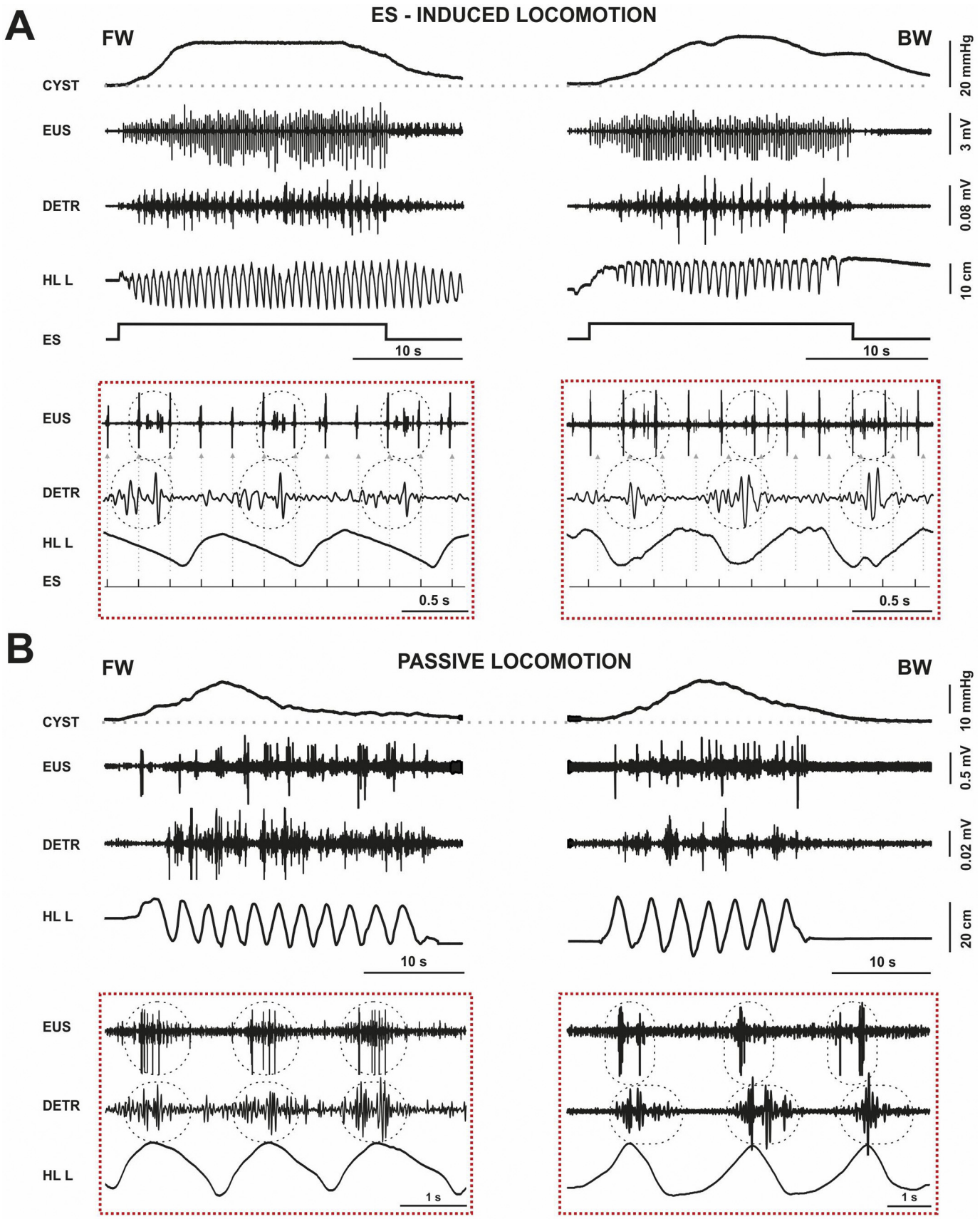

Fig. 2. An activity of the lower urinary tract: EMG signals of the detrusor (DETR) and external urinary sphincter (EUS), and cystometry (CYST)) during ES-evoked (A) and passive (B) forward (FW) and backward (BW) locomotion. Red countered images are enlarged parts of the top rows. HL L – anterior-posterior movements of the left hindlimb, ES – epidural stimulation. (For interpretation of the references to colour in this figure legend, the reader is referred to the web version of this article.)

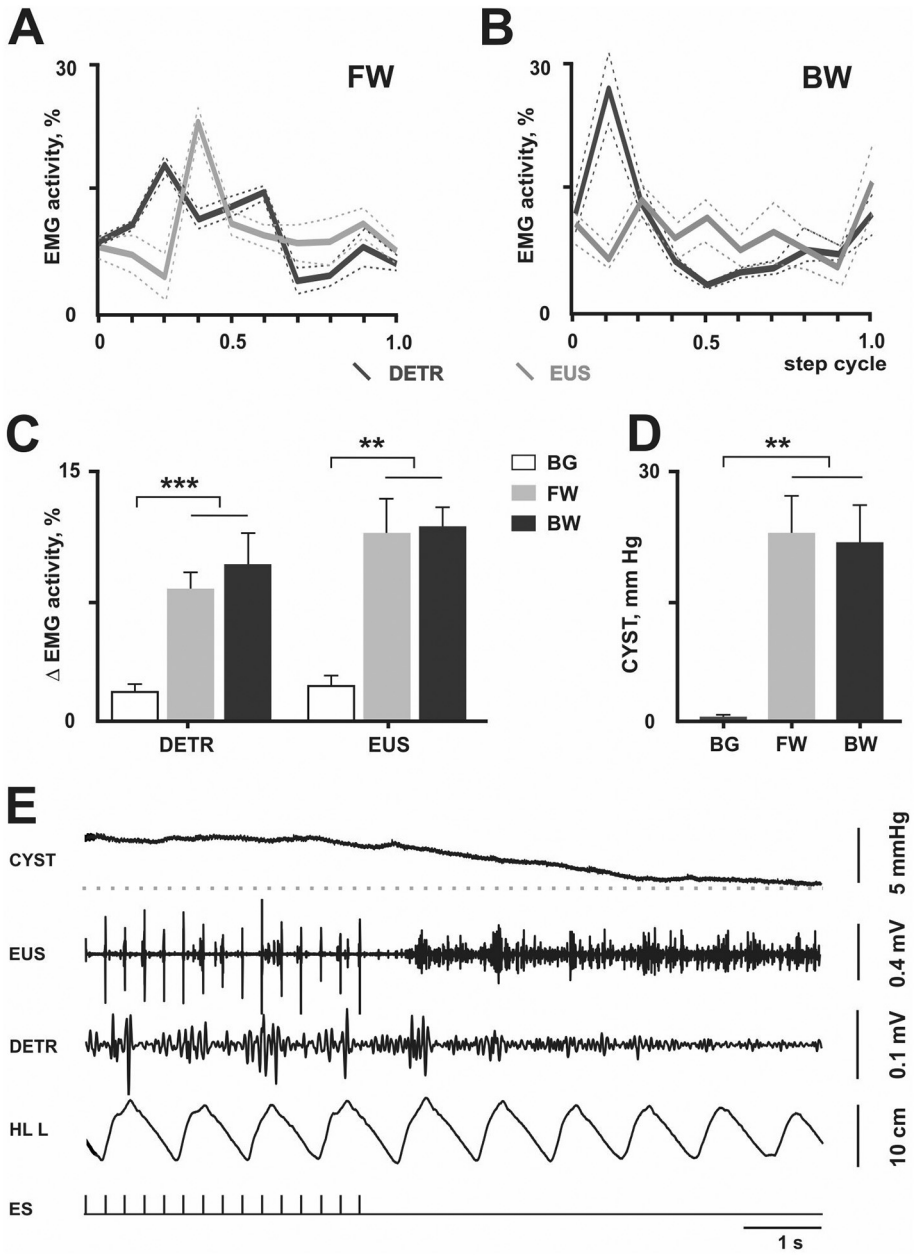

Fig. 3. Step-related activity of the lower urinary tract during ES-evoked forward (FW) and backward (BW) locomotion. A, B – averaged (1 SE, dotted line) EMG signals in the detrusor (DETR, dark gray) and external urinary sphincter (EUS, light gray) over the step cycle (n = 10 steps were averaged for each stepping session in one cat). Dashed lines are SEM. C – difference between the maximal and minimal signal level of the EMG signals of the DETR (dark gray) and EUS (light gray) during FW and BW locomotion, and during background activity (BG) (n = 8 cats). D – level of the averaged increment of the cystometric signal (CYST) during FW and BW locomotion (n = 8 cats). E – effect of ES cessation to the LUT activity. *, **, *** – $p < 0.05$; $p < 0.01$; $p < 0.001$.

(10 gait cycles were averaged for each stepping session), an EMG activity of the detrusor had a clear modulation during the step cycle (Fig. 3A, B), for both FW and BW locomotion; as for the EUS, this was rather observed for the FW not BW locomotion. For the estimation of the averaged dependence of the EMG of the LUT over the locomotion in all cats tested (n = 8), a difference between the maximal and minimal EMG activities during FW and BW locomotion, and before locomotion (background, BG) was assessed. Both detrusor and EUS had larger values of this parameter (Fig. 3C), comparing with the background activity; this difference was valid for the detrusor (7.92 ± 0.87 *vs* 1.68 ± 0.30; $p = 0.0002$) and EUS (11.23 ± 1.80 *vs* 1.96 ± 0.52; $p = 0.0007$) as during FW stepping, as during BW one (detrusor, 9.30 ± 2.03 *vs* 1.68 ± 0.30; $p = 0.0079$, EUS, 11.61 ± 1.16 *vs* 1.96 ± 0.52; $p = 0.0159$). Such modulation pattern of the LUT EMG activity was followed by the 30-fold increase of the intravesical pressure both for FW and BW locomotion (Fig. 3D). After ES cessation the EUS and detrusor modulation pattern continued for a few seconds along with the facilitation state of the spinal locomotor network and limb stepping (Fig. 3E). Note, that the tonic baseline as well as bursting EMG activity in EUS increased and became more high frequency when the detrusor activity deteriorated and intravesical pressure reduced. This EUS-detrusor antagonism is well correspondent to the previously described coordinated contraction / relaxation of these LUT muscles evoked by the electrical stimulation of the superficial parts of the dorsolateral funiculus at the level of the segments L5-L6 of the spinal cord of the decerebrate cat (Fedirchuk and Shefchyk, 1991).

3.2. *Activated visceral neurons within the sacral spinal cord of the stepping cats*

The relationship of the bladder and hindlimb activation patterns suggests that the spinal visceral network became active during stepping. To prove this we used *c-fos* technique to find out neuronal population in the sacral segments activated in the course of locomotion. For this task we chosen two different locomotor modes (Buford et al., 1990): FW and BW stepping having variously distributed networks in the spinal cord (Merkulyeva et al., 2018).

We have shown earlier that FW and BW locomotion have different

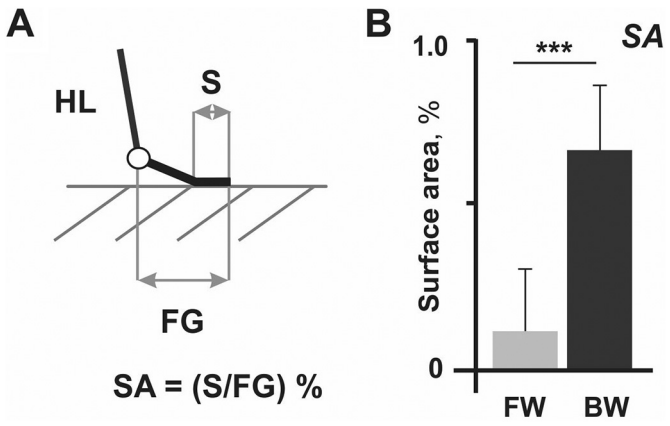

Fig. 4. A size of the relative support surface area (SA) of the foot, in cats stepping forward (FW) and backward (BW). HL – hindlimb. A – a scheme for the counting of the SA. B – value for the FW and BW stepping. *** – $p < 0.001$.

kinematic features including significantly different angle of the ankle joint during foot placement (Merkulyeva et al., 2018). Since the spinal neuronal network controlling bladder is located in the close relation to the motoneuronal pools of the foot and fingers muscles (Vanderhorst and Holstege, 1997) we expect BW and FW stepping lead to the different activation level of the corresponding spinal networks by the different somatosensory feedback from the foot. We compared a relative support surface area (SA) of the foot assessed as a percent of the total length of the foot contacting surface, during FW and BW locomotion (Fig. 4A) and found the significantly higher level of SA in the cats stepping BW (0.21 ± 0.04 *vs* 0.66 ± 0.13; $p = 0.00045$) (Fig. 4B).

To analyze the pattern of the activated spinal visceral neurons after FW and BW stepping, we used a *c-fos* immunostaining technique. Many FOS+ neurons (from 54 to 230 *per* side of the spinal cord) were visualized within the spinal segment S2, but obviously, only part of them were visceral. Thereby, we had to outline a region of the gray matter devoted to the visceral control. This outlining must meet the following requests: be simple and standard for all slices and cats used. In cats, neurons devoted to the visceral control are organized within the sacral spinal cord into several groups. Parasympathetic autonomic neurons are located within the sacral parasympathetic nucleus (SPN), in the dorsal gray commissure (DGC), and in area extending along the lamina I curvature (de Groat and Yoshimura, 2010) (Fig. 5A). Somatic neurons controlling external urinary sphincter (EUS) are located within the so-called Onuf's nucleus located within the ventrolateral part of the ventral horn (Kuzuhara et al., 1980; Schrøder, 1981; Vanderhorst and Holstege, 1997). We suppose that the Onuf's nucleus was not labelled in our experiment since (1) it is located rostrally to the bladder parasympathetic preganglionic cells (Vanderhorst and Holstege, 1997), but we did not observe FOS+ cells in a presumptive location of the Onuf's nucleus in segment S1 and in the rostral part of the S2 segment. (2) As it was shown in our (Merkulyeva et al., 2018) and in other papers (Huang et al., 2000; Dai et al., 2005) somatic motoneurons are rarely labelled by the *c-fos*. Thereafter Onuf's cells are unlikely to be labelled in our experiment.

We compared Descartes coordinates of FOS+ nuclei with those of labelled neurons after HRP injection to the pelvic nerve (Nadelhaft et al., 1980; Morgan et al., 1979), after preliminary alignment of countered images in our and literature data, in relation to the central canal and gray matter boundaries (Fig. 5B). A good correspondence (89.7 ± 6.4%) was revealed between the spatial location of the HRP neurons and FOS+ nuclei located within the lateral regions of the gray matter where SPN cells were obtained (Nadelhaft et al., 1980; Morgan et al., 1979).

We also used an immunostaining of NO-synthase and Ca^{2+}-binding protein calretinin to attribute the activated cells to the specific visceral pathways. Sacral preganglionic parasympathetic areas are marked by NO-synthase (NOS) (Nadelhaft et al., 1980; Morgan et al., 1979), and a correspondence between NOS+ and FOS+ cells was also revealed here (Fig. 5C). Weaker correspondence (23.6 ± 15.4%) was shown between the spatial location of the HRP neurons and FOS+ nuclei within the area just dorsally to the central canal (Fig. 5B). This area is spatially correspondent to the location of the DGC nucleus. Since it was shown that DGC neurons expressed Ca^{2+}-binding protein calretinin (Ren and Ruda, 1994), we also used this marker to outline the DGC (Fig. 5D).

Based upon HRP, *c-fos*, calretinin, and NOS labelling, we geometrically subdivided gray matter by parallel vertical and parallel horizontal lines passed through the simple landmarks as ventral median fissure, protrusion of the white matter into the lateral gray matter (point A). The line *v1* was drawn through the ventral median fissure; the line *v2* – parallel to *v1* through the point A. The line *h1* was perpendicular to the lines *v1* and *v2* (crossed them at points B and A respectively). The line *h2* was tangent through the protrusion of the white matter into the ventral gray (point C) and was perpendicular to the lines *v1* and *v2* (and crosses line *v2* at point D). The line *h3* was parallel to the lines *h1* and *h2* and crossed the center of the central canal (point F). The line *v3* was parallel to *v1* and *v2* through the midpoint of the distance between point A and B (point G). Line *o1* connected points D and G, and crossed line *h3* in a point H. Line *o2* connected points C and H. As a result, the intermediate gray matter and a lateral part of the ventral horns were subdivided into three regions of interest bordered by the points A, I, H, and G (Fig. 5E, pink; centrolateral area, CL); by points I, E, D, and H (Fig. 5E, red; ventrolateral area, VL), and by points H, F, B, and G (Fig. 5E, dark gray; pericanal area, PC). Two first ones, both corresponded to groupings of neurons labelled after HRP injection into pelvic nerve and were possibly related to the cells processed for afferents from large intestine and lower urinary tract, respectively (dorsal band and lateral band; (Nadelhaft et al., 1980; Morgan et al., 1979). Region VL also contained labelled cells after HRP injection into the bladder wall (Vanderhorst and Holstege, 1997). The third region (PC) presumably contained the DGC neurons. Within the dorsal horns, it was difficult to clearly extract a visceral area, since neurons received afferents from the lower urinary tract occupied mainly the thin lateral area curved in parallel to the laminae I; and since bladder afferents have not been detected in the center of the dorsal horn (laminae III-IV) (Nadelhaft et al., 1980; Morgan et al., 1979; de Groat et al., 2001; de Groat and Yoshimura, 2010), thus we subdivided dorsal region into lateral (DL) and medial (DM) regions (Fig. 5E, gray and light gray areas). The remaining region of the gray matter mostly contained laminae VIII and IX where it is difficult to precisely outline the visceral areas.

Approximately 63–84% of FOS+ nuclei located within areas DL, CL, VL, and PC supposed to be visceral (63–84% in cats stepping FW, and 69–80% in cats stepping BW) (Fig. 6A-B). In control animal, fewer FOS+ nuclei were obtained within the segment S2 (94 *vs* 122–262 (in FW cats) and *vs* 133–394 (BW cats)), the number of FOS+ nuclei localized within the visceral areas was 88%. Only in cats stepping BW, FOS+ nuclei were organized into well-developed clusters contributing to areas CL and VL (Fig. 6A-B), but FOS+ nuclei were also present in these areas in cats stepping FW. Since an inter-individual variability in the number of the FOS+ nuclei was observed, a percent numbers of the FOS+ nuclei were analyzed. A significant difference between cats stepping FW and BW was observed for the percent number of the FOS+ nuclei located in area VL (5.37 ± 0.68 *vs* 10.46 ± 0.89; $p = .0022$) (Fig. 6D).

We should note that in experiment, stepping was evoked by the ES (Fig. 1B) of different loci of the spinal cord (located from the rostral part of the segment L5 to the middle part of the segment L7), and a possible relationship between the number of the FOS+ nuclei and the location of the ES electrode can be assumed. However, we didn't reveal any clear linkage between them, both for general number of the FOS+

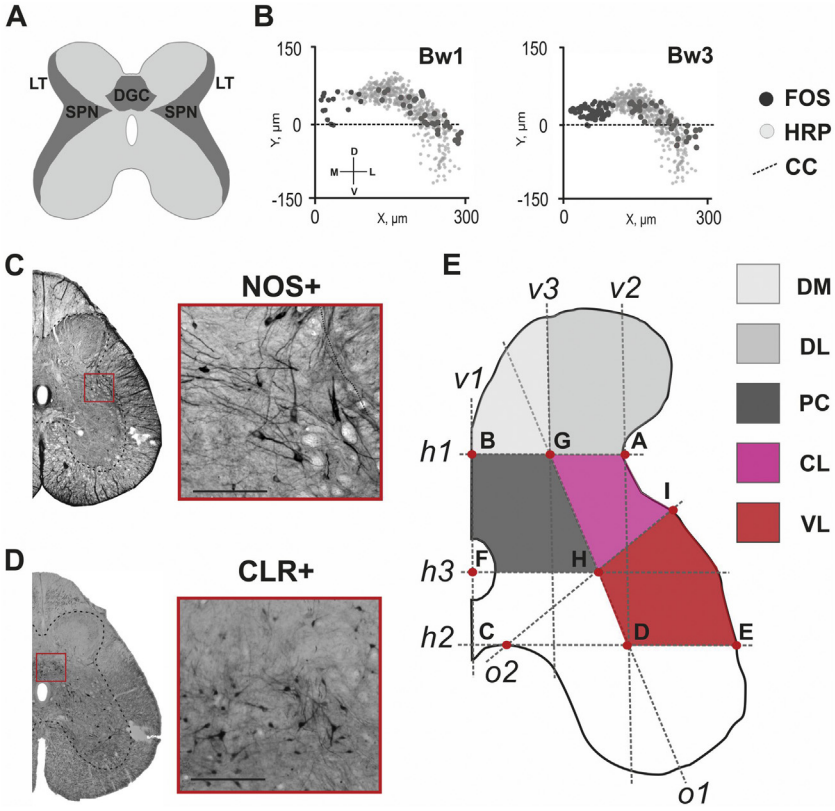

Fig. 5. The method for the division of the sacral spinal cord gray matter. A – a schematic view of the visceral areas within the transverse slice of the spinal cord. DGC – dorsal gray commissure, SPN – sacral parasympathetic nucleus, LT – Lissauer tract. B – a superposition of FOS + nuclei (marked by dark gray) with the HRP-labelled cells (from Morgan et al., 1979; Nadelhaft et al., 1980; Vanderhorst and Holstege, 1997) (marked by light gray), within the same Descartes coordinates, in two cats (Bw1 and Bw3). All cells were centered in relation to the central canal having coordinates [0; 0]. C, D – a transverse slices of the segment S2, stained for calretinin (C) and NO-synthase (D). Groups of the calretinin-labelled (CLR +) neurons and NO-synthase-labelled cells (NOS +) are presented in enlarged inserts. Calibration marker at C, D is 200 µm. E – a scheme for the gray matter subdivision. Italic letters v1, v2, v3, h1, h2, h3, o1, and o2 – basic lines. Solid letters A-I – basic points. DM, DL, PC, CL, and VL – areas of interest.

nuclei (Fig. 6E) and the percent number of the FOS + nuclei within the area VL (Fig. 6F).

4. Discussion

The present work provides direct evidences of the visceral network activation during ES-evoked locomotion. *At first*, we observed that stepping of the cats induces the bursts in the EMG activity of the detrusor and EUS well matched to the locomotor rhythm. According to the current knowledge based on neurophysiological recordings (Gaunt et al., 2006; Gerasimenko et al., 2006) and computer simulations (Rattay et al., 2000; Capogrosso et al., 2013), the mechanisms underlying the facilitation of motor activity with ES engages the spinal circuits by recruiting dorsal root fibers carrying somatosensory signals from the limbs at their entry into the spinal cord as well as along the longitudinal portions of the fiber trajectories (Gerasimenko et al., 2008; Musienko et al., 2011). Although it cannot be excluded the direct influence of the ES to spinal visceral pathways, we found that the EMG bursts in detrusor and EUS muscle were not followed the frequency of ES and could continue for a few seconds after cessation of ES (Fig. 2A, Fig. 3E). Moreover, similar LUT activation pattern was obtained during passive hindlimbs movements without ES. These evidences suggest that the obtained effect of bladder activation was rather influenced from the processing of the sensorimotor signals during stepping by the spinal somato-visceral integrative network.

Secondly, we investigated a gene *c-fos* expression in visceral areas of the spinal cord during locomotion and shown that many of the FOS + nuclei in segment S2 located within three areas (PC, VL, and CL) of intermediate gray matter relating to the visceral control. As shown in cats and rats, the afferent pathways from the pelvic visceral organs project into Lissauer's tract, invade the lamina I curvature and pass into laminae V-VII and X (Birder and de Groat, 1992; de Groat et al., 2001). The most pronounced part of this projection is a lateral pathway. It terminates in the SPN located within the centrolateral area, and also sends collaterals to the DGC (Nadelhaft et al., 1980; Morgan et al., 1979; Honda et al., 1983). It should be noted that the SPN consists of two different parts, one of them (the "lateral band" of the SPN) contains neurons lying along the lateral edge of the intermediate gray in lamina VII and innervating the urinary bladder, and the second one (the "dorsal band" of the SPN) contains neurons lying across the base of the dorsal horn in laminae V-VI and innervating the large intestine (Nadelhaft et al., 1980; Morgan et al., 1979; de Groat et al., 1981). Our way of the gray matter division generally allows to distinguish these two parts of the SPN. The "lateral band" is presumably located in VL area, and the "dorsal band", within the CL area.

The total pattern of the *c-fos* labeling was quite similar to those obtained after electrical stimulation of visceral afferent pathways in the pelvic nerve (Birder and de Groat, 1992) as well as after irritation of the low urinary tract (Cruz et al., 1994; Birder et al., 1999; Vizzard, 2000) and proximal colon (Lanteri-Minet et al., 1993; Martínez et al., 1998). Moreover, neurons located near the central canal are influenced by activity in both somatic and visceral afferent fibers (Honda, 1985). Thus, we can assume that locomotor activity evoked by ES directly or indirectly activated the integrative networks received both somatic and visceral primary afferent inputs.

Thirdly, the total number of the FOS + cells in area VL is dependent upon the locomotor mode (FW or BW stepping), and we obtained a greater number of activating neurons within the bladder-related ventrolateral area after BW stepping. It confirms that activating locomotor network itself involves the specific visceral population of neurons of VL area and that some aspects of the BW stepping can stronger influence the sacral parasympathetic network by the reflex or biomechanical mechanisms. BW stepping was characterized by the larger surface support area of the foot comparing to FW one, and spinal neuronal network controlling bladder is located in the close relation to the motoneuronal pools of the foot muscles (Vanderhorst and Holstege, 1997); therefore possibly, the somatosensory input from the foot is specifically affects the visceral neurons attributed to the bladder control. Similar effect of somatovisceral influence was obtained on patients with SCI (Chen et al., 2015), electrical stimulation of somatic afferent nerves in

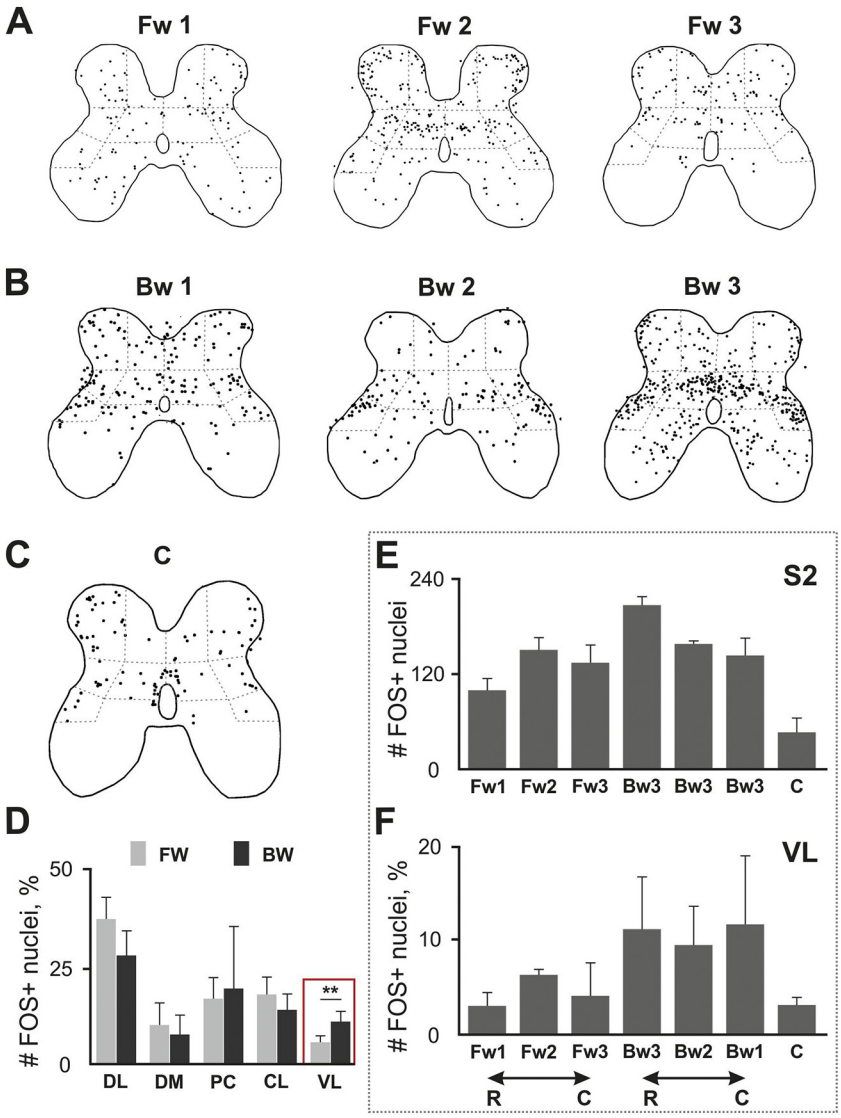

Fig. 6. Distribution of the c-fos-immunopositive (FOS+) nuclei within the gray matter of the spinal cord. A-C – total views of the sacral slices (as a sum of 5 slices, see Methods) with FOS+ nuclei (nuclei are marked by dots), in cats stepping forward (FW) (A), stepping backward (BW) (B), and in control cat (C) (C). At A-C, the thin dotted lines outline the boundaries of the areas of interest. D – a percent number of FOS+ nuclei in areas of interest (DL, DM, PC, CL, and VL) in cats stepping FW and BW. ** – $p < 0.01$. E, F – a dependence of the total number of FOS+ nuclei in segment S2 (E) and a percent number of the FOS+ neurons in area VL (F) upon the location of the ES electrode, in individual cats stepping FW, BW, and in control cat. R, C – rostral and caudal directions of the lumbar area.

the foot increased the bladder capacity in neurogenic bladder.

In sum, the present work confirms that the somatovisceral integrating mechanisms, at least, for bladder, are carried out on the spinal cord level. This supports the opinion that locomotor training and spinal cord stimulation of sensorimotor circuitry can be important for recovery of visceral control including LUT function of the patients with SCI (Gad et al., 2014; Pettigrew et al., 2017). Further studies of the spinal network related to the integrative sensorimotor and visceral control will help to optimize the neurorehabilitation strategies and to develop the spinal neuroprosthetics interfaces for clinical applications.

5. Conclusions

We found that stepping of a decerebrate cat is accompanied by involvement of the urinary system. *C-fos* technique allowed to see that many activated neurons were localized within several visceral areas of the S2 segment gray matter matched the sacral parasympathetic nucleus and the dorsal gray commissure. Cats stepping BW, in comparison to the cats stepping FW, had 4-fold more *c-fos*-immunopositive nuclei within the ventrolateral part of the sacral parasympathetic nucleus apparently correspondent to the “lateral band” contained cells controlling bladder function. The present work provides the direct evidences of visceral neurons activation depending on the specific of locomotor pattern and confirms the somatovisceral integration carrying out on the spinal cord level.

Acknowledgements

The study was supported by Russian Foundation for Basic Research (RFBR grants №17-04-01822, №17-29-01034-ofi_m, №19-015-00409).

References

Bahns, E., Ernsberger, U., Jänig, W., Nelke, A., 1986. Functional characteristics of lumbar visceral afferent fibres from the urinary bladder and the urethra in the cat. Pflugers Arch. 407, 510–518. https://doi.org/10.1007/BF00657509.

Birder, L.A., de Groat, W.C., 1992. Increased c-fos expression in spinal neurons after irritation of the lower urinary tract in the rat. J. Neurosci. 12, 4878–4889. https://doi.org/10.1523/JNEUROSCI.12-12-04878.1992.

Birder, L.A., Roppolo, J.R., Erickson, V.L., de Groat, W.C., 1999. Increased c-fos expression in spinal lumbosacral projection neurons and preganglionic neurons after irritation of the lower urinary tract in the rat. Brain Res. 834, 55–65. https://doi.org/10.1016/S0006-8993(99)01546-2.

Buford, J.A., Zernicke, R.F., Smith, J.L., 1990. Adaptive control for backward quadrupedal walking I. Posture and hindlimb kinematics. J. Neurophysiol. 64, 745–755. https://doi.org/10.1152/jn.1990.64.3.745.

Capogrosso, M., Wenger, N., Raspopovic, S., Musienko, P., Beauparlant, J., Luciani, L.B., Courtine, G., Micera, S., 2013. A computational model for epidural electrical stimulation of spinal sensorimotor circuits. J. Neurosci. 33, 19326–19340. https://doi.org/10.1523/JNEUROSCI.1688-13.2013.

Chen, G., Liao, L., Miao, D., 2015. Electrical stimulation of somatic afferent nerves in the foot increases bladder capacity in neurogenic bladder patients after sigmoid cystoplasty. BMC Urol. 15, 26. https://doi.org/10.1186/s12894-015-0023-8.

Courtine, G., Gerasimenko, Y., van den Brand, R., Yew, A., Musienko, P., Zhong, H., Song, B., Ao, Y., Ichiyama, R.M., Lavrov, I., Roy, R.R., Sofroniew, M.V., Edgerton, V.R., 2009. Transformation of nonfunctional spinal circuits into functional states after the loss of brain input. Nat. Neurosci. 12, 1333–1342. https://doi.org/10.1038/nn.2401.

Cruz, F., Avelino, A., Lima, D., Coimbra, A., 1994. Activation of the c-fos proto-oncogene in the spinal cord following noxious stimulation of the urinary bladder. Somatosens. Mot. Res. 11, 319–325. https://doi.org/10.3109/08990229409028876.

Dai, X., Noga, B.R., Douglas, J.R., Jordan, L.M., 2005. Localization of spinal neurons activated during locomotion using the c-fos immunohistochemical method. J. Neurophysiol. 93, 3442–3452. https://doi.org/10.1152/jn.00578.2004.

de Groat, W.C., 1995. Mechanisms underlying the recovery of lower urinary tract function following spinal cord injury. Spinal Cord 33, 493–505. https://doi.org/10.1038/sc.1995.109.

de Groat, W.C., Yoshimura, N., 2010. Changes in afferent activity after spinal cord injury. Neurourol. Urodyn. 29, 63–76. https://doi.org/10.1002/nau.20761.

de Groat, W.C., Nadelhaft, I., Milne, R.J., Booth, A.M., Morgan, C., Thor, K., 1981. Organization of the sacral parasympathetic reflex pathways to the urinary bladder and large intestine. J. Auton. Nerv. Syst. 3, 135–160. https://doi.org/10.1016/0165-1838(81)90059-X.

de Groat, M.O., Fraser, M., Yoshiyama, S., Smerin, C., Tai, M.B., Chancellor, N., Yoshimura, J.R., Roppolo, W., 2001. Neural control of the urethra. Scand. J. Urol. Nephrol. 35, 35–43. https://doi.org/10.1080/003655901750174872.

Dragunow, M., Faull, R., 1989. The use of c-fos as a metabolic marker in neuronal pathway tracing. J. Neurosci. Methods 29, 261–265. https://doi.org/10.1016/0165-0270(89)90150-7.

Duru, P.O., Tillakaratne, N.J., Kim, J.A., Zhong, H., Stauber, S.M., Pham, T.T., Xiao, M.S., Edgerton, V.R., Roy, R.R., 2015. Spinal neuronal activation during locomotor-like activity enabled by epidural stimulation and 5-hydroxytryptamine agonists in spinal rats. J. Neurosci. Res. 93, 1229–1239. https://doi.org/10.1002/jnr.23579.

Fedirchuk, B., Shefchyk, S.J., 1991. Effects of electrical stimulation of the thoracic spinal cord on bladder and external urethral sphincter activity in the decerebrate cat. Exp. Brain Res. 84, 635–642. https://doi.org/10.1007/BF00230976.

Fry, C.H., Wu, C., Sui, G.P., 1998. Electrophysiological properties of the bladder. Int. Urogynecol. J. Pelvic Floor Dysfunct. 9, 291–298. https://doi.org/10.1007/BF01901509.

Gad, P.N., Roy, R.R., Zhong, H., Lu, D.C., Gerasimenko, Y.P., Edgerton, V.R., 2014. Initiation of bladder voiding with epidural stimulation in paralyzed, step trained rats. PLoS ONE 9, e108184. https://doi.org/10.1371/journal.pone.0108184.

Gad, P.N., Roy, R.R., Zhong, H., Gerasimenko, Y.P., Taccola, G., Edgerton, V.R., 2016. Neuromodulation of the neural circuits controlling the lower urinary tract. Exp. Neurol. 285, 182–189. https://doi.org/10.1016/j.expneurol.2016.06.034.

Gaunt, R.A., Prochazka, A., Mushahwar, V.K., Guevremont, L., Ellaway, P.H., 2006. Intraspinal microstimulation excites multisegmental sensory afferents at lower stimulus levels than local alpha-motoneuron responses. J. Neurophysiol. 96, 2995–3005. https://doi.org/10.1152/jn.00061.2006.

Gerasimenko, Y.P., Lavrov, I.A., Courtine, G., Ichiyama, R.M., Dy, C.J., Zhong, H., Roy, R.R., Edgerton, V.R., 2006. Spinal cord reflexes induced by epidural spinal cord stimulation in normal awake rats. J. Neurosci. Methods 157, 253–263. https://doi.org/10.1016/j.jneumeth.2006.05.004.

Gerasimenko, Y., Roy, R.R., Edgerton, V.R., 2008. Epidural stimulation: comparison of the spinal circuits that generate and control locomotion in rats, cats and humans. Exp. Neurol. 209, 417–425. https://doi.org/10.1016/j.expneurol.2007.07.015.

Gerasimenko, Y., Musienko, P., Bogacheva, I., Moshonkina, T., Savochin, A., Lavrov, I., Roy, R.R., Edgerton, V.R., 2009. Propriospinal bypass of the serotonergic system that can facilitate stepping. J. Neurosci. 29, 5681–5689. https://doi.org/10.1523/JNEUROSCI.6058-08.2009.

Gomez-Amaya, S.M., Barbe, M.F., De Groat, W.C., Brown, J.M., Tuite, G.F., Corcos, J., Fecho, S.B., Braverman, A.S., Ruggieri Sr., M.R., 2015. Nat. Rev. Urol. 12, 100–118. https://doi.org/10.1038/nrurol.2015.4.

Grillner, S., 1980. Can mammalian pattern generators be understood? Behav. Brain Sci. 3, 549–550. https://doi.org/10.1017/S0140525X00006713.

Guttmann, L., Whitteridge, D., 1947. Effects of bladder distension on autonomic mechanisms after spinal cord injuries. Brain 70, 361–404. https://doi.org/10.1093/brain/70.4.361.

Honda, C.N., 1985. Visceral and somatic afferent convergence onto neurons near the central canal in the sacral spinal cord of the cat. J. Neurophysiol. 53, 1059–1078. https://doi.org/10.1152/jn.1985.53.4.1059.

Honda, C.N., Rethelyi, M., Petrusz, P., 1983. Preferential immunohistochemical localization of vasoactive intestinal polypeptide (VIP) in the sacral spinal cord of the cat: light and electron microscopic observations. J. Neurosci. 3, 2183–2196. https://doi.org/10.1523/JNEUROSCI.03-11-02183.1983.

Horst, M., Heutschi, J., van den Brand, R., Andersson, K.E., Gobet, R., Sulser, T., Courtine, G., Eberli, D., 2013. Multisystem neuroprosthetic training improves bladder function after severe spinal cord injury. J. Urol. 189, 747–753. https://doi.org/10.1016/j.juro.2012.08.200.

Huang, A., Noga, B.R., Carr, P.A., Fedirchuk, B., Jordan, L.M., 2000. Spinal cholinergic neurons activated during locomotion: localization and electrophysiological characterization. J. Neurophysiol. 83, 3537–3547. https://doi.org/10.1152/jn.2000.83.6.3537.

Ichiyama, R.M., Courtine, G., Gerasimenko, Y.P., Yang, G.J., van den Brand, R., Lavrov, I.A., Zhong, H., Roy, R.R., Edgerton, V.R., 2008. Step training reinforces specific spinal locomotor circuitry in adult spinal rats. J. Neurosci. 28, 7370–7375. https://doi.org/10.1523/JNEUROSCI.1881-08.2008.

Iwahara, T., Atsuta, Y., Garcia-Rill, E., Skinner, R.D., 1992. Spinal cord stimulation-induced locomotion in the adult cat. Brain Res. Bull. 28, 99–105. https://doi.org/10.1016/0361-9230(92)90235-P.

Kruse, M.N., De Groat, W.C., 1993. Spinal pathways mediate coordinated bladder/urethral sphincter activity during reflex micturition in decerebrate and spinalized neonatal rats. Neurosci. Lett. 152, 141–144. https://doi.org/10.1016/0304-3940(93)90503-d.

Kuzuhara, S., Kanazawa, I., Nakanishi, T., 1980. Topographical localization of the Onuf's nuclear neurons innervating the rectal and vesical striated sphincter muscles: a retrograde fluorescent double labeling in cat and dog. Neurosci. Lett. 16, 125–130. https://doi.org/10.1016/0304-3940(80)90331-6.

Lanteri-Minet, M., Isnardon, P., De Pommery, J., Menetrey, D., 1993. Spinal and hindbrain structures involved in visceroception and visceronociception as revealed by the expression of Fos, Jun and Krox-24 proteins. Neuroscience 55, 737–753. https://doi.org/10.1016/0306-4522(93)90439-M.

Martínez, V., Wang, L., Mayer, E., Taché, Y., 1998. Proximal colon distention increases Fos expression in the lumbosacral spinal cord and activates sacral parasympathetic NADPHd-positive neurons in rats. J. Comp. Neurol. 390, 311–321. https://doi.org/10.1002/(SICI)1096-9861(19980119)390:3<311::AID-CNE1>3.0.CO;2-4.

Merkulyeva, N., Veshchitskii, A., Makarov, F., Gerasimenko, Y., Musienko, P., 2016. Distribution of 28 kDa calbindin-immunopositive neurons in the cat spinal cord. Front. Neuroanat. 9, 166. https://doi.org/10.3389/fnana.2015.00166.

Merkulyeva, N., Veshchitskii, A., Gorsky, O., Pavlova, N., Zelenin, P.V., Gerasimenko, Y., Deliagina, T.G., Musienko, P., 2018. Distribution of spinal neuronal networks controlling forward and backward locomotion. J. Neurosci. 38, 4695–4707. https://doi.org/10.1523/JNEUROSCI.2951-17.2018.

Minassian, K., Jilge, B., Rattay, F., Pinter, M.M., Binder, H., Gerstenbrand, F., Dimitrijevic, M.R., 2004. Stepping-like movements in humans with complete spinal cord injury induced by epidural stimulation of the lumbar cord: electromyographic study of compound muscle action potentials. Spinal Cord 42, 401–416. https://doi.org/10.1038/sj.sc.3101615.

Morgan, C., Nadelhaft, I., de Groat, W.C., 1979. Location of bladder preganglionic neurons within the sacral parasympathetic nucleus of the cat. Neurosci. Lett. 14, 189–194. https://doi.org/10.1016/0304-3940(79)96146-9.

Musienko, P.E., Bogacheva, I.N., Gerasimenko, Y.P., 2007. Significance of peripheral feedback in the generation of stepping movements during epidural stimulation of the spinal cord. Neurosci. Behav. Physiol. 37, 181–190. https://doi.org/10.1007/s11055-007-0166-5.

Musienko, P., van den Brand, R., Maerzendorfer, O., Larmagnac, A., Courtine, G., 2009. Combinatory electrical and pharmacological neuroprosthetic interfaces to regain motor function after spinal cord injury. IEEE Trans. Biomed. Eng. 56, 2707–2711. https://doi.org/10.1109/tbme.2009.2027226.

Musienko, P., van den Brand, R., Märzendorfer, O., Roy, R.R., Gerasimenko, Y., Edgerton, V.R., Courtine, G., 2011. Controlling specific locomotor behaviors through multidimensional monoaminergic modulation of spinal circuitries. J. Neurosci. 31, 9264–9278. https://doi.org/10.1523/JNEUROSCI.5796-10.2011.

Musienko, P.E., Zelenin, P.V., Lyalka, V.F., Gerasimenko, Y.P., Orlovsky, G.N., Deliagina, T.G., 2012. Spinal and supraspinal control of the direction of stepping during locomotion. J. Neurosci. 32, 17442–17453. https://doi.org/10.1523/JNEUROSCI.3757-12.2012.

Nadelhaft, I., de Groat, W.C., Morgan, C., 1980. Location and morphology of parasympathetic preganglionic neurons in the sacral spinal cord of the cat revealed by retrograde axonal transport of horseradish peroxidase. J. Comp. Neurol. 193, 265–281. https://doi.org/10.1002/cne.901930118.

Pettigrew, R.I., Heetderks, W.J., Kelley, C.A., Peng, G.C., Krosnick, S.H., Jakeman, L.B., Egan, K.D., Marge, M., 2017. Epidural spinal stimulation to improve bladder, bowel, and sexual function in individuals with spinal cord injuries: a framework for clinical research. IEEE Trans. Biomed. Eng. 64, 253–262. https://doi.org/10.1109/TBME.2016.2637301.

Presley, R.W., Menetrey, D., Levine, J.D., Basbaum, A.I., 1990. Systemic morphine suppresses noxious stimulus-evoked Fos protein-like immunoreactivity in the rat spinal cord. J. Neurosci. 10, 323–335. https://doi.org/10.1523/JNEUROSCI.10-01-00323.1990.

Rattay, F., Minassian, K., Dimitrijevic, M.R., 2000. Epidural electrical stimulation of posterior structures of the human lumbosacral cord. 2. Quantitative analysis by computer modeling. Spinal Cord 38, 473–489. https://doi.org/10.1038/sj.sc.3101039.

Ren, K., Ruda, M.A., 1994. A comparative study of the calcium-binding proteins calbindin-D28K, calretinin, calmodulin and parvalbumin in the rat spinal cord. Brain Res. Rev. 19, 163–179. https://doi.org/10.1016/0165-0173(94)90010-8.

Schindelin, J., Arganda-Carreras, I., Frise, E., Kaynig, V., Longair, M., Pietzsch, T., Preibisch, S., Rueden, C., Saalfeld, S., Schmid, B., Tinevez, J.Y., White, D.J., Hartenstein, V., Eliceiri, K., Tomancak, P., Cardona, A., 2012. Fiji: an open-source platform for biological-image analysis. Nat. Methods 9, 676–682. https://doi.org/10.1038/nmeth.2019.

Schrøder, H.D., 1981. Onuf's nucleus X: a morphological study of a human spinal nucleus. Anat. Embryol. (Berl.) 162, 443–453. https://doi.org/10.1007/BF00301870.

Shefchyk, S.J., Buss, R.R., 1998. Urethral pudendal afferent-evoked bladder and sphincter reflexes in decerebrate and acute spinal cats. Neurosci. Lett. 244, 137–140. https://doi.org/10.1016/S0304-3940(98)00155-4.

Shik, M.L., Orlovsky, G.N., 1976. Neurophysiology of locomotor automatism. Physiol. Rev. 56, 465–501. https://doi.org/10.1152/physrev.1976.56.3.465.

Shkorbatova, P.Y., Lyakhovetskii, V.A., Merkulyeva, N.S., Veshchitskii, A.A., Bazhenova, E.Y., Laurens, J., Pavlova, N.V., Musienko, P.E., 2018. Prediction algorithm of the cat spinal segments lengths and positions in relation to the vertebrae. Anat. Rec. https://doi.org/10.1002/ar.24054. (Epub ahead of print).

Vanderhorst, V.G., Holstege, G., 1997. Organization of lumbosacral motoneuronal cell groups innervating hindlimb, pelvic floor, and axial muscles in the cat. J. Comp. Neurol. 382, 46–76. https://doi.org/10.1002/(SICI)1096-9861(19970526)382:1<46::AID-CNE4>3.0.CO;2-K.

Vizzard, M.A., 2000. Alterations in spinal cord Fos protein expression induced by bladder stimulation following cystitis. Am. J. Phys. Regul. Integr. Comp. Phys. 278, R1027–R1039. https://doi.org/10.1152/ajpregu.2000.278.4.R1027.

Whelan, P.J., 1996. Control of locomotion in the decerebrate cat. Prog. Neurobiol. 49, 481–515. https://doi.org/10.1016/0301-0082(96)00028-7.